Surface Science 649 (2016) 27–33

Contents lists available at ScienceDirect

Surface Science

journal homepage: www.elsevier.com/locate/susc

# Theoretical investigation of surface states and energetics of PtSi surfaces

Manish K. Niranjan *

*Department of Physics, Indian Institute of Technology, Hyderabad, India*

ARTICLE INFO

*Article history:*
Received 18 October 2015
Accepted 23 January 2016
Available online 2 February 2016

*Keywords:*
Silicide
Surface electronic structure
Surface energies
Work functions
Ab initio calculations

ABSTRACT

Platinum silicide (PtSi) is highly promising material for applications in microelectronic devices. In this article, the surface electronic structure, surface energetics and work functions of stoichiometric and non-stoichiometric PtSi(010) surfaces are explored within the framework of first-principle density functional theory. The surface rumpling is found to be significant only for the top surface layer. The computed values of the rumpling parameter for the top three layers are ~11.0%, ~0.9% and ~1.9%. Further, the interlayer relaxation is found to be largest for the top layer and decreases rapidly for inner layers. Localized surface states are obtained in the valence band at ~9.0 eV below the Fermi level. Under rich Pt and Si growth conditions, nonstoichiometric (010) terminations are found to have the lowest surface energies, whereas stoichiometric termination has the lowest surface energy (~1.74 J/m$^2$) under mixed conditions. The work function of stoichiometric (010) termination is computed to be 5.15 eV and differ as much as by ±0.5 eV for nonstoichiometric terminations.



## 1. Introduction

Metal silicides are highly promising materials for applications in silicon microelectronics [1–12]. Silicides with semiconducting properties have been found promising for applications in photovoltaics [13], optoelectronics [14] and as thermoelectric materials [15]. In addition to technological applications, silicides also exhibit diverse physical properties which make them attractive from solely scientific perspective. Silicides of iron, cobalt and manganese are now understood to be highly correlated electronic materials [16]. Furthermore, interesting phenomena such as quantum non-Fermi liquid behavior and critical phase transition have been observed in manganese silicide [17,18]. Metal silicides are used in complimentary metal-oxide-semiconductor (CMOS) devices to form Ohmic contacts, gate electrode and local interconnects due to their low contact resistance to Si, low resistivity, good thermal stability, and excellent process compatibility with standard Si technology. Over the years, titanium, cobalt and nickel silicides have been used in CMOS device manufacturing. However, these silicides exhibit large Schottky barrier at the silicon–silicide interface which results in relatively high contact resistance. In recent years, silicides of platinum have been found promising for application as contact materials in nanoscale CMOS devices due to their low Schottky barrier to *p*-type silicon and excellent thermal stability [2,3,19,20]. Besides application as contact materials in silicon-based semiconductor devices, platinum silicides have also been successfully used in Schottky-barrier photodiodes (SBD) and detectors [1,2]. For instance, PtSi/*n*-Si junction based photodiode have found applications in multi-wavelength pyrometry and infrared (IR) imaging system. Schottky-barrier detectors are more advantageous over *p*–*n* junctions based detectors in that they are more robust in harsh radiation environments and are less prone to wear [21]. Furthermore, SBD are easy to integrate with Schottky-bipolar circuits which in turn provide superior radiation resistance.

During platinum silicidation reaction, two stable compositions, PtSi and $Pt_2Si$, are known to form in Pt-Si intermixed layers [20]. In the first reaction, Pt diffuses into Si resulting in the formation of intermediate compound $Pt_2Si$. Subsequently, in the second reaction, stable PtSi is formed as Si diffuses into $Pt_2Si$. Despite their technological importance, very few theoretical studies of platinum-silicides have been reported. In particular, not much is known about their surface electronic structure and surface energetics. Recently, we reported a first-principles study of Schottky barrier height at Si/PtSi(010) interface [22]. In this article, we present a detailed study of surface electronic structure and surface energies of stoichiometric and nonstoichiometric PtSi(010) surfaces. In addition, we also study the effect of surface defects on surface energies, work functions and electronic structure of PtSi(010) surfaces. The (010) termination is interesting in that it has low surface energy and promising for epitaxial growth of PtSi on Si substrate [5,23,24]. The knowledge of work function dependence on surface orientation and surface defects is important as it may have important implications for device applications [4,6]. We also discuss the performance of LDA and GGA correlational functionals with regard to various computed parameters.

The rest of the paper is organized as follows. In Section 2, computational methodology is presented. In Section 3, the crystal and electronic

* Tel.: +91 40 23016092; fax: +91 40 23016032.
*E-mail address:* manish@iith.ac.in.

http://dx.doi.org/10.1016/j.susc.2016.01.019
0039-6028/

structure of PtSi are reviewed. The surface electronic structure of PtSi(010) surfaces are presented in Section 4. Surface energies and work functions are discussed in Section 5. Concluding remarks are given in Section 6.

## 2. Computational methodology

The calculations are performed using projected augmented wave (PAW) potentials within the framework of density functional theory as implemented in the VASP package [25]. The local-density approximation (LDA) and Pedew–Burke–Ernzerhof (PBE) form of generalized gradient approximation (GGA) are employed for exchange-correlation potentials [26,27]. The Kohn–Sham wavefunctions are expanded in plane wave basis set with a kinetic energy cutoff of 400 eV. The Brillouin zone of bulk PtSi is sampled using an $8 \times 12 \times 8$ Monkhorst–Pack $k$-point mesh. Self-consistency in calculations is achieved until the total energies are converged to $10^{-6}$ eV/cell. The structures are relaxed until the largest force becomes less than $10^{-2}$ eV/Å. Surfaces are simulated using supercells with different number of PtSi(010) and vacuum layers. Symmetric slabs based on $(1 \times 1)$ surface cells are used with in-plane lateral lattice constants fixed to bulk values. Brillouin zone integrations are performed using $6 \times 1 \times 6$ (or more) Monkhorst–Pack mesh and supercells are relaxed along growth direction until the forces on each atom is reduced to 0.01 eV/Å or less.

## 3. Crystal and electronic structure of bulk PtSi

PtSi crystallizes in a primitive orthorhombic structure with *Pnma* space group symmetry (#62 in the International X-ray Tables) [28]. The unit cell consist four symmetry-equivalent Pt and four symmetry equivalent Si atoms. The Pt and Si atoms are located on (010) plane at $b/4$ and $3b/4$ positions. The computed and experimental lattice constants, fractional atomic coordinates, cohesive energy and heat of formation of PtSi are presented in Table 1. The fractional atomic coordinates of Pt and Si atoms are indicated as $u_{Si}$, $u_{Pt}$, $v_{Si}$ and $v_{Pt}$ for Si and Pt atoms. As can be seen from Table 1, the computed lattice constants and fractional atomic coordinates are in good agreement (~1%–2%) with previously reported theoretical and experimental values [22,28]. As expected, LDA and GGA computed values of lattice constants are underestimated and overestimated, respectively, as compared to experimental values. Further, the LDA and GGA computed cohesive energies are larger by ~19% and ~1% than experimental values. It may be noted that the LDA (GGA) are known to overestimate (underestimate) the value of cohesive energy of metals by ~20% and 5%, respectively [29]. Next, we summarize the electronic structure of bulk PtSi. The energy bands of bulk PtSi along high symmetry directions in the Brillouin zone are shown in Fig. 1. The total and partial density of states (DOS) for PtSi are shown in Fig. 2. As can be seen, the states at the Fermi level in PtSi are derived primarily from 5*d* orbitals of Pt. The DOS in PtSi at the Fermi level are reduced significantly as compared to those in bulk Pt. This is indicative of poor metallic properties of PtSi as compared to that of pure bulk Pt. The reduction of DOS at Fermi energy in PtSi is expected due to Si mixing in pure Pt. As will be discussed in Section 5, low DOS at the Fermi energy in PtSi have implications for lower work functions of PtSi surfaces as compared to those for pure Pt surfaces. It is also clear from Fig. 1 and 2 that Pt 5*d* bands are relatively delocalized and contribute to entire valence band. The atomic structure

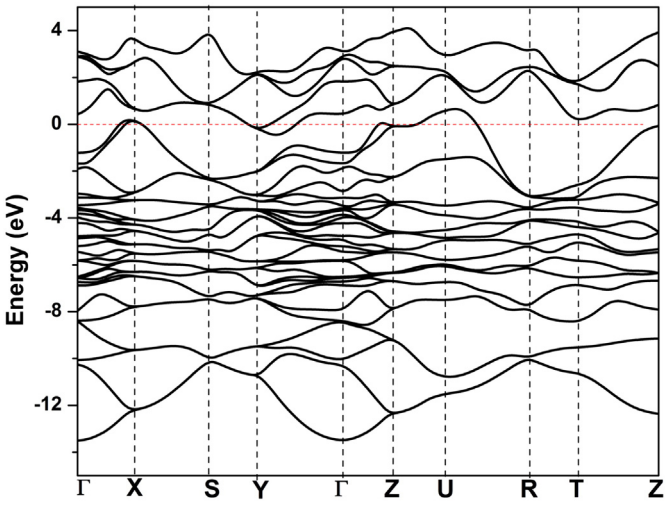


**Fig. 1.** Computed (LDA) energy band structure of bulk PtSi along high symmetry directions in the Brillouin zone of orthorhombic structure.

of PtSi(010) surface is shown in Fig. 3. The valence charge density contours for this surface is shown in Fig. 4. As can be seen, the Pt and Si atoms form directional three center (Pt-Si-Pt) bonds in PtSi. Overall, the bonding in PtSi can be described as mixed covalent-metallic.

## 4. Surface electronic structure of PtSi(010) surfaces

Next, we study surface electronic structure of PtSi (010) surface. The PtSi(010) surface is stoichiometric (see Fig. 3) and has relatively low surface energy. Further, PtSi(010) is suitable for epitaxial growth on Si(001) substrate due to small misfit strain. The stoichiometric PtSi(010)-$(1 \times 1)$ surface unit cell has two Pt and two Si atoms. After relaxation, the PtSi(010) surface layers exhibit rumpling due to unequal forces acting on surface atoms (Pt and Si). The difference in forces acting on surface atoms may be understood as arising due to difference in atomic polarizability. The inward force is generally weaker on anions than on cations. The rumpling parameter $\delta r_i$ is defined as

$$\delta r_i = \left(r_i^{Pt} - r_i^{Si}\right)/d_0 \tag{1}$$

where $r_i^{Pt(Si)}$ are coordinates of Pt (Si) atoms in the $i$th layer along the [010] direction and $d_0$ is bulk interlayer separation. Table 2 lists the computed rumpling parameter in PtSi(010) supercells composed of 13, 17, 21 and 25 layers. The LDA (GGA) computed values of the rumpling parameter for the top three layers($\delta r_1, \delta r_2, \delta r_3$) are obtained to be 11.0% (10.5%), 0.9% (1.5%) and 1.9% (1.8%) for a supercell with 25 layers. This suggests that rumpling is significant only for the top surface layer. The magnitude of rumpling (~11% or ~0.2 Å) for the top PtSi(010) surface is comparable to that calculated for many binary semiconductor (GaAs) surfaces [30]. Table 2 also shows the results for percentage interlayer relaxation for unreconstructed stoichiometric PtSi(010) surface layers in supercells consisting 13, 15, 21 and 25 layers. As can be seen, the LDA (GGA) computed interlayer spacing ($\Delta d_{12}$) between top two layers (in 25 layer supercell) exhibits a contraction of 5.46% (5.51%).

**Table 1**
Computed (LDA and GGA) and experimental lattice constants (Å), fractional atomic coordinates, cohesive energy ($E_{Coh}$), heat of formation ($\Delta H_f$) of bulk PtSi.

| | $a$ | $b$ | $c$ | $u_{Pt}$ | $v_{Pt}$ | $u_{Si}$ | $v_{Si}$ | $E_{Coh}$ (eV/atom) | $\Delta H_f$ (eV/atom) |
|---|---|---|---|---|---|---|---|---|---|
| LDA | 5.561 | 3.588 | 5.896 | 0.9983 | 0.1920 | 0.1783 | 0.5842 | 7.0 | 0.72 |
| GGA | 5.665 | 3.621 | 5.986 | 0.9951 | 0.1934 | 0.1781 | 0.5825 | 5.9 | 0.66 |
| Exp.[a] | 5.575 | 3.586 | 5.922 | 0.9956 | 0.1922 | 0.177 | 0.583 | 5.85 | 0.62 |

[a] Ref. [40].